# Effects of Zn substitution for Cu on superconducting and normal-state properties of $(La,Sr)_2CuO_4$, $(Nd,Ce,Sr)_2CuO_4$, and $(Nd,Ce)_2CuO_4$

S. Ikegawa,* T. Yamashita, T. Sakurai, R. Itti, H. Yamauchi, and S. Tanaka
*Superconductivity Research Laboratory, International Superconductivity Technology Center, 10-13 Shinonome 1-chome, Koto-ku, Tokyo 135, Japan*
(Received 30 August 1990)

Superconducting and normal-state properties of Zn-doped samples of $La_{1.85}Sr_{0.15}Cu_{1-x}Zn_xO_{4-\delta}$ ($T$ phase), $Nd_{1.4}Ce_{0.2}Sr_{0.4}Cu_{1-x}Zn_xO_{4-\delta}$ ($T^*$ phase), and $Nd_{1.85}Ce_{0.15}Cu_{1-x}Zn_xO_{4-\delta}$ ($T'$ phase) are investigated for Zn content $x$ in the range of 0–0.04. Zn doping alters the lattice parameters for the $T$ and $T^*$ phases but does not for the $T'$ phase. For all of the $T$, $T^*$, and $T'$ phases, $T_c$, the Meissner signal, and the shielding signal monotonically decrease for increasing $x$. From the magnetic-susceptibility measurement, it is suspected that isolated Cu spins are induced around doped Zn in the $T$ phase. As the Zn content increases, the magnitude of the Hall coefficient decreases in both $T$ and $T'$ phases, while the carrier density, estimated from a chemical analysis, remains constant. Possible mechanisms for this are discussed.

## I. INTRODUCTION

In the superconducting cuprates, $[CuO_2]$ planes have been regarded as essential for the occurrence of superconductivity. Moreover, localized spins on Cu ions and the short-range two-dimensional antiferromagnetic correlations between the spins have also been considered to be important. The existence of such localized spins and antiferromagnetic-like correlations between the localized spins were confirmed by neutron diffraction[1] even in the superconducting phases. In order to study the spin contribution to superconductivity, it is useful to investigate the Zn substitution effect in cuprate superconductors. Indeed, the Zn substitution is expected not to alter the carrier density but to affect the spin correlation through the spin vacancies on the Zn sites. Previous work for $(La,Sr)_2CuO_4$,[2] $YBa_2Cu_3O_7$,[3] and Bi-Sr-Ca-Cu-O (Ref. 4) showed that the Zn substitution suppressed the superconducting transition temperature $T_c$ more effectively than substitution by other transition metals, which had magnetic moments. Therefore, $T_c$ suppression due to $3d$-metal substitution is most likely not caused by a pair-breaking effect by the magnetic moments of $3d$ metals,[2–4] as was the case of the Abrikosov and Gor'kov model. In $YBa_2Cu_3O_7$, it was reported that when the hole concentration derived from the measured Hall coefficient increased upon Zn doping beyond an optimum value, $T_c$ decreased.[3,5] However, the origin of excess holes is unknown. The Zn-substitution effect for $La_{1.85}Sr_{0.15}CuO_{4-\delta}$ ($T$ phase) was investigated by Xiao *et al.*[6] They concluded that the suppression of $T_c$ was due to the filling of the local Cu $d_{x^2-y^2}$ states by $Zn^{2+}$ ($d^{10}$), which hindered the Cu $3d$ holes from becoming itinerant. However, how the local-state filling affects the transport and magnetic properties in the normal state is unknown.

Recently, two new superconducting cuprates which had a crystal structure similar to the $T$-phase compounds have been discovered. One was $(Nd,Ce,Sr)_2CuO_{4-\delta}$ ($T^*$ phase).[7] The other was the $T'$ phase which contained electrons as charge carriers.[8] Symmetric behaviors in the magnetic, transport, and optical properties upon carrier doping were reported[9] between the electron-doped superconductors ($T'$ phase) and the hole-doped superconductors ($T$ phase). Moreover, according to neutron-scattering experiments,[10] the Cu spins in the electron-doped superconductors behaved similarly to those in the hole-doped superconductors. The substitution effects for Cu were studied for the $T'$ phase[11–14] but none has been reported for the $T^*$ phase.

To compare the substitution effects for the three different phases $T$, $T^*$, and $T'$ is important because these phases contain layers of copper oxide octahedra, pyramids, and squares, respectively, as the electronically active structural components. Each of these phases has only one kind of site which accommodates small-sized ions (including Cu and those that substitute for Cu). This is the reason why the present work deals only with the three phases. In this paper, we investigate Zn-substitution effects for $T$, $T^*$, and $T'$ compounds in order to elucidate the spin-vacancy contributions on the magnetic and transport properties. Superconducting properties and normal-state properties are investigated for polycrystalline samples of the three phases.

## II. EXPERIMENTS

All the samples were prepared by a standard solid-state reaction method using high-purity powders of $La_2O_3$ (99.9% purity), $SrCO_3$ (99.9% purity), $Nd_2O_3$ (99.99% purity), $CeO_2$ (99.9% purity), CuO (99.99% purity), and ZnO (99.9% purity). Appropriate powders were mixed for nominal compositions of $La_{1.85}Sr_{0.15}Cu_{1-x}Zn_xO_{4-\delta}$ ($T$ phase), $Nd_{1.4}Ce_{0.2}Sr_{0.4}Cu_{1-x}Zn_xO_{4-\delta}$ ($T^*$ phase), and $Nd_{1.85}Ce_{0.15}Cu_{1-x}Zn_xO_{4-\delta}$ ($T'$ phase) for $x=0$, 0.01, 0.015, 0.02, 0.03, or 0.04 by means of a ball mill using ethanol. In order to have dopants uniformly distributed, calcinings and regrindings were repeated. For the $T$

 

phase, the mixed powder was calcined at 900–1000 °C for a total of 50 h in air with three intermediate regrindings. The calcined powder was sintered at 1050 °C for 50 h in $O_2$ flow. In order to maximize the oxygen content, the samples were slowly cooled down at a rate of 60 °C/h from the sintering temperature and were finally annealed at 500 °C for 10 h in $O_2$ flow. For the $T^*$ phase, the mixed powder was calcined at 900–1150 °C for a total of 60 h with five intermediate regrindings. The samples were reground again and pressed into rectangular bars, and sintered at 1150 °C for 10 h followed by annealing at 500 °C for 10 h. All heating processes except for the first calcining were done in $O_2$ flow for the preparation of the $T^*$ phase. For the $T'$ phase, the mixed powder was calcined at 950–1000 °C for a total of 60 h in air with five intermediate regrindings. The calcined powder was sintered at 1100 °C for 30 h in $O_2$ flow and post annealed at 1050 °C for 15 h in $N_2$ flow, and then quenched from 1050 °C to room temperature in the same atmosphere. Finally, the sample was annealed at 500 °C for 10 h in $N_2$ flow in order to decrease resistivity, as reported by Takagi, Uchida, and Tokura.[15]

The phases present and lattice constants were determined by powder x-ray diffraction using Cu $K\alpha$, radiation. In order to observe the uniformity of dopant distribution in the $T'$ samples, electron probe microanalysis (EPMA) was used. The oxygen content of the $T$ samples was analyzed by an iodometric titration technique improved by Nazzal *et al.*[16] The oxygen content of the $T'$ phase was analyzed by an inert gas fusion nondispersive ir method (HORIBA: model EMGA-650) because the iodometric titration technique faced difficulties because of the mixed valence of Ce ions.

Resistivity measurements were carried out by a conventional dc four-probe method in the temperature range between 1.6 and 300 K. Resistivity was also measured under an applied magnetic field using a 10-T superconducting solenoid. Hall coefficients at temperatures between $T_c$ and 300 K were measured by using an automatic unit, in which a superconducting solenoid and a 10-nV resolution digital voltmeter were installed. The maximum applied field was 6 T and the maximum applied current was 50 mA. The temperature was kept constant within ±0.2 K during one sequence of measurements, including reversing operations of the magnetic field and the current direction. The temperature was measured by means of a calibrated Pt sensor as well as a carbon-glass resistance sensor. For the Hall measurements, pellet samples were thinned to the dimension of $7\times2\times0.15$ $mm^3$. The electrical contacts for the $T$ and $T^*$ samples were made using gold paste which underwent a heat treatment at 900 °C. The electrical contacts for $T'$ phase were formed using In solder.

The dc magnetic susceptibility was measured using a SQUID magnetometer (Quantum Design model—MPMS). For superconducting properties, measurements were done in an applied field of 1 mT. For normal-state susceptibility, fields of 2, 0.5, and 0.5 T were applied for the $T$, $T^*$, and $T'$ phases, respectively. The measured samples were so slender that the demagnetizing factor was negligibly small (less than 0.08). Errors in the normal-state susceptibility due to a demagnetizing field were estimated to be less than 0.5%. Electron-spin-resonance measurements were performed using a microwave of 9.1 GHz in the applied field of 0.33±0.15 T at 295 K. A photoemission study was done to investigate the valence state of doped ions [x-ray photoemission spectroscopy (XPS)] and the valence-band spectra [ultraviolet photoemission spectroscopy (UPS)].

## III. RESULTS AND DISCUSSION

### A. Structural chemistry

First of all, we show the results of powder x-ray diffraction. Figures 1(a)–1(c) show the lattice parameters $a$ and $c$ in terms of the dopant concentration $x$ of the three phases, all of which have tetragonal crystal structures. $La_{1.85}Sr_{0.15}Cu_{1-x}Zn_xO_{4-\delta}$ samples were of single phase for $x=0.0$–$0.03$. The term "single phase" means that no single unindexed peak with an intensity larger than 0.5% of the main peak is observed in a diffraction pattern. In the $T$ phase [Fig. 1(a)], the $a$ axis increases and the $c$ axis decreases with increasing $x$ up to 0.03, as previously reported by Xiao *et al.*[6] The $x$ dependence of lattice constants [Fig. 1(a)] and of magnetic susceptibility (as will be shown later in Fig. 8) suggest that Zn was not completely substituted for Cu in the sample with $x=0.04$. From the XPS measurements, the intensity of the Zn $2p$ peak increases linearly as $x$ increases up to $x=0.04$.[17]

Samples of $Nd_{1.4}Ce_{0.2}Sr_{0.4}Cu_{1-x}Zn_xO_{4-\delta}$ with $x=0$–$0.015$ have the $T^*$ structure and are single phase. The $T'$ phase and $CeO_2$ are observed as secondary phases in samples with $x>0.02$. For $Nd_{1.4}Ce_{0.2}Sr_{0.4}Cu_{1-x}Zn_xO_{4-\delta}$, the $a$ axis increases and the $c$ axis decreases with increasing $x$, as shown in Fig. 1(b).

Samples of $Nd_{1.85}Ce_{0.15}Cu_{1-x}Zn_xO_{4-\delta}$ with $x=0$ $-0.015$ have a single-phase $T'$ structure. As an impurity phase, $Nd_{0.25}Ce_{0.75}O_{1.875}$ [No. 28-226 in the powder diffraction file (PDF) of Joint Committee on Powder Diffraction Standards (JCPDS) (Ref. 18)] or $Nd_{0.5}Ce_{0.5}O_{1.75}$ [No. 28-267 in the PDF of JCPDS (Ref. 18)] are observed with the intensity ratio of 0.7, 1.2, and 2.7 % for the samples with $x=0.02$, 0.03, and 0.04, respectively. In the $T'$ phase, the lattice parameters $a$ and $c$ are not changed by Zn substitution as shown in Fig. 1(c), which contrasts with the case of the $T$ and $T^*$ phases. The data are consistent with earlier reports.[11–14] In order to check the possibility of precipitation or segregation of Zn, we studied all the samples of the $T'$ phase by EPMA. In each of the samples with $x=0$, 0.01, 0.015, and 0.02, Zn is distributed uniformly. In the samples with $x=0.03$ and 0.04, islands of a few $\mu$m diameter are observed in which the concentration of Zn is greater by a factor of 5 than the bulk. The Meissner signal [which will be shown later in Fig. 2(c)] changes continuously with increasing $x$ up to $x=0.015$. Therefore, in our samples, Zn is probably substituted for Cu uniformly up to $x=0.015$.

When $Cu^{2+}$ ions occupy the $B$ sites of the $K_2NiF_4$ structure, the oxygen octahedron is elongated along the $c$

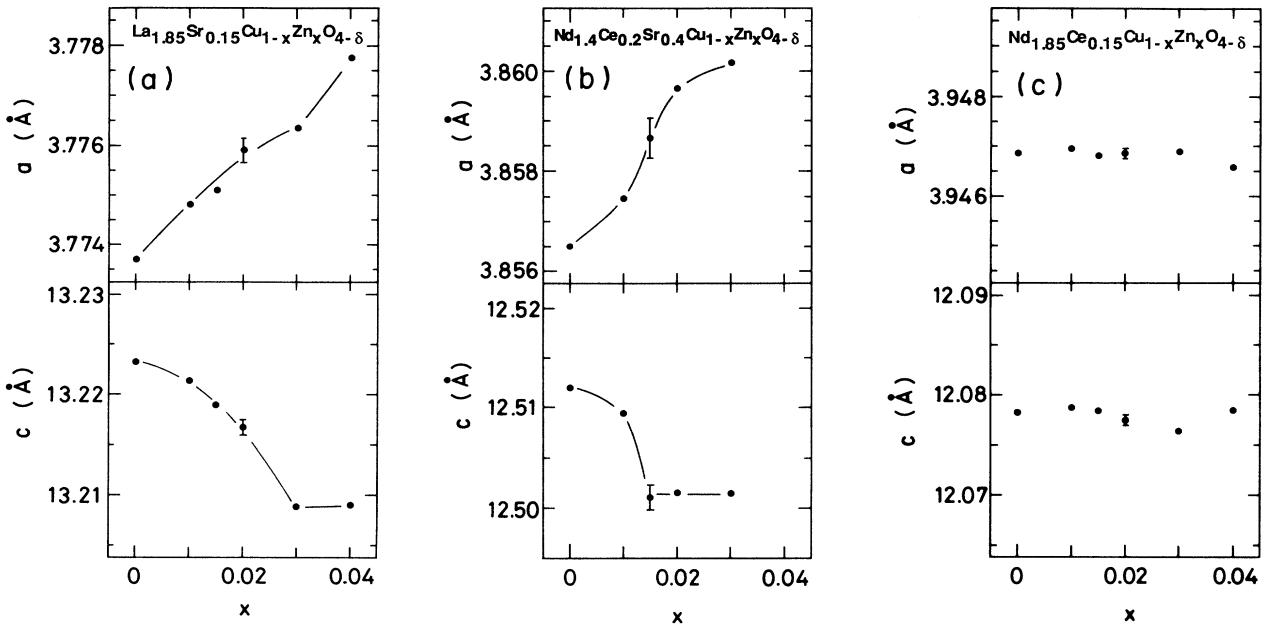


FIG. 1. Tetragonal unit-cell parameters $a$ and $c$ vs the Zn content $x$ for (a) $La_{1.85}Sr_{0.15}Cu_{1-x}Zn_xO_{4-\delta}$ (b) $Nd_{1.4}Ce_{0.2}Sr_{0.4}Cu_{1-x}Zn_xO_{4-\delta}$, and (c) $Nd_{1.85}Ce_{0.15}Cu_{1-x}Zn_xO_{4-\delta}$. All the curves are guides for the eyes.

axis and compressed along the $a$ axis, and the $d\gamma$ orbital is split into two different levels by the Jahn-Teller effect. The substitution for $Cu^{2+}$ in this environment by $Zn^{2+}$, which has a filled $d$ shell and is not a Jahn-Teller ion, probably relaxes Jahn-Teller distortions. Therefore, in the $T$ phase, the $a$ axis increases and the $c$ axis decreases upon Zn substitution. This speculation was first proposed by Xiao *et al.*[6] The change in the lattice parameters of the $T^*$ phase, which has a pyramidal coordination of oxygen around copper, is probably due to the same effect. If one accepts this discussion of the Jahn-Teller effect, the constant lattice parameters observed for the $T'$ phase on Zn substitution may be explained as follows. The crystal structure of the $T'$ phase is similar to that of the $T$ phase; however, the position of the apical oxygen in the $T$ phase is shifted in the $T'$ phase. Hence, in the $T'$ phase, whichever transition-metal ions occupy the $B$ site, the $d\gamma$ orbital splits widely into two levels by analogy with the square four-coordination case. Therefore, Jahn-Teller distortions or relaxations cannot occur around $Cu^{2+}$ or $Zn^{2+}$ in the $T'$ phase. Thus, the lattice parameters are not significantly changed by the replacement of $Cu^{2+}$ by ions having nearly the same radius (i.e., $Zn^{2+}$).

Henceforth, we are concerned only with the single-phase regions in the three systems: $x=0$–$0.03$ for the $T$ phase, $x=0$–$0.015$ for the $T^*$ phase, and $x=0$–$0.015$ for the $T'$ phase.

### B. Superconducting properties

Figure 2 shows dc magnetic susceptibility measured for the $T$ [Fig. 2(a)], $T^*$ [Fig. 2(b)], and $T'$ phases [Fig. 2(c)] with decreasing temperature. $T_c$'s were determined at the onset of the Meissner signal and are plotted in Fig. 3. $T_c$ decreases as increasing Zn content ($x$) in the $T$, $T^*$, and $T'$ phases. The slopes $dT_c/dx$ in Fig. 3 are nearly identical, being about $-12$ K/(at. % replacement of Cu) for the $T$, $T^*$, and $T'$ phases. The Zn substitution affects not only $T_c$ but also the magnitude of diamagnetic signal as seen in Fig. 2. In Fig. 4 the ratio of diamagnetic signal $\chi_M$ at 5 K to a full Meissner effect ($=-1/4\pi$ in cgs) is plotted as a function of $x$. The ratio decreases rapidly with increasing $x$ for all the $T$, $T^*$, and $T'$ phases. This phenomenon was observed in many other cases of substitution of Cu.[4,6,12–14]

The increase in the density of flux trapped in the sample during field cooling, induced by an increase in the macroscopic pinning force, can diminish the Meissner signal.[19] The magnitude of $J_c$ was estimated for $La_{1.85}Sr_{0.15}CuO_{4-\delta}$ and $La_{1.85}Sr_{0.15}Cu_{0.985}Zn_{0.015}O_{4-\delta}$ from the hysteresis loops of magnetization versus field ($\pm 5.5$ T) using the Bean critical-state model. It was found that the magnitude of $J_c$ decreases by 1 order of magnitude upon Zn doping. We measured the magnetic susceptibility with increasing temperature after zero-field cooling; that is, the shielding effect. Figure 5 shows the ratio of the shielding signal at 5 K to a full Meissner effect. Not only the Meissner signal but also the shielding signal rapidly decrease with increasing Zn content.

The hysteresis-loop and shielding-effect data suggest that the decrease in Meissner signal is not due to the increase in the pinning force but to an increase in the normal-state portion of the sample as the Zn content increased. This might be related to the model proposed by Junod *et al.*[20] in which the pairing potential fluctuates spatially on the scale of the lattice parameter as a result of small chemical perturbations (e.g., atomic substitution). It should be noted that the $x$ value, i.e., Zn con-

tent, where $T_c$ becomes zero is in good agreement with that where both the Meissner signal and the shielding signal vanished. The superconducting volume fraction appears to decrease linearly from 100% for the sample with $x=0$ to 0% for the sample with $x=0.03$ for the case of the $T$ phase. Similarly, for the case of the $T^*$ and $T'$ phases, it appears to decrease from 100% for the sample with $x=0$ to 0% for the sample with $x=0.015$. If superconductivity is assumed to be destroyed in a local area of a disk shape in the $[CuO_2]$ plane around every Zn ion distributed uniformly, the radius of the disk-shape area can be 12 and 18 Å for the $T$ and $T'$ ($T^*$) phases, respec-

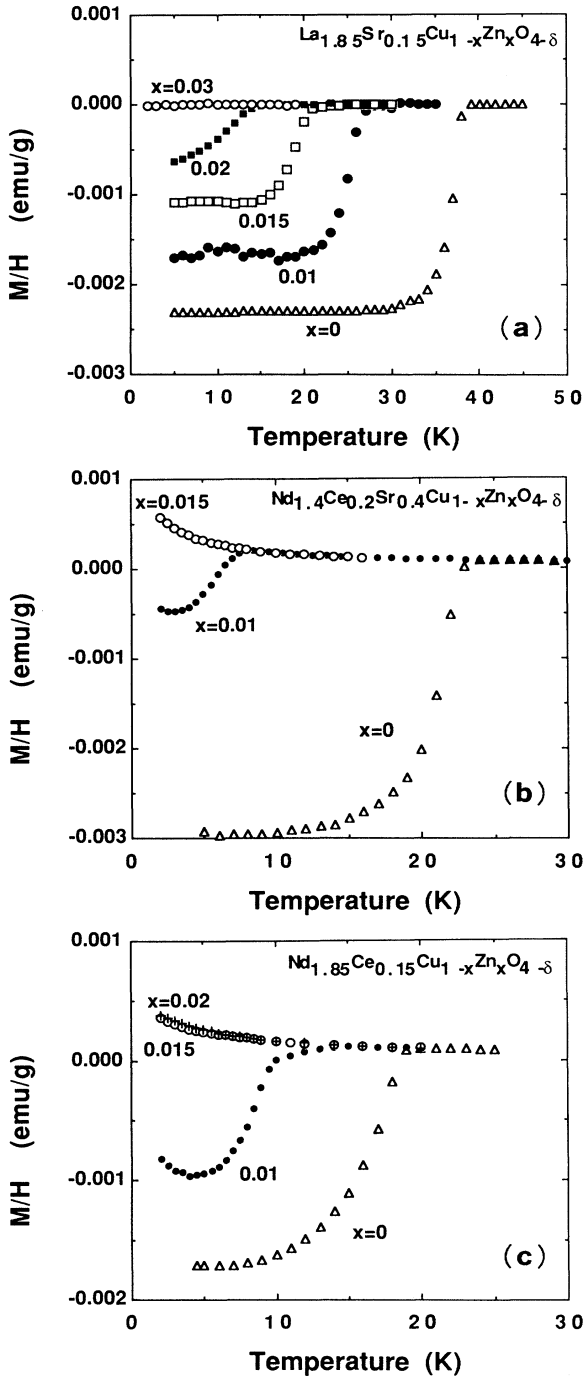


FIG. 2. Superconducting diamagnetic susceptibility (Meissner effect) for (a) $La_{1.85}Sr_{0.15}Cu_{1-x}Zn_xO_{4-\delta}$, (b) $Nd_{1.4}Ce_{0.2}Sr_{0.4}Cu_{1-x}Zn_xO_{4-\delta}$, and (c) $Nd_{1.85}Ce_{0.15}Cu_{1-x}Zn_xO_{4-\delta}$.

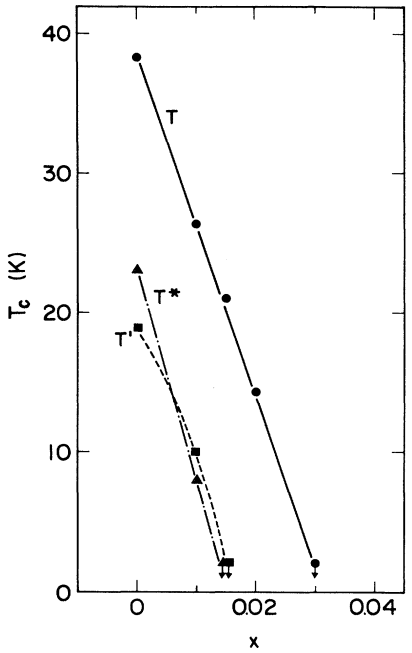


FIG. 3. The dependence of $T_c$ on the Zn content $x$ for $La_{1.85}Sr_{0.15}Cu_{1-x}Zn_xO_{4-\delta}$ ($T$), $Nd_{1.4}Ce_{0.2}Sr_{0.4}Cu_{1-x}Zn_xO_{4-\delta}$ ($T^*$), and $Nd_{1.85}Ce_{0.15}Cu_{1-x}Zn_xO_{4-\delta}$ ($T'$). All the curves are guides for the eyes.

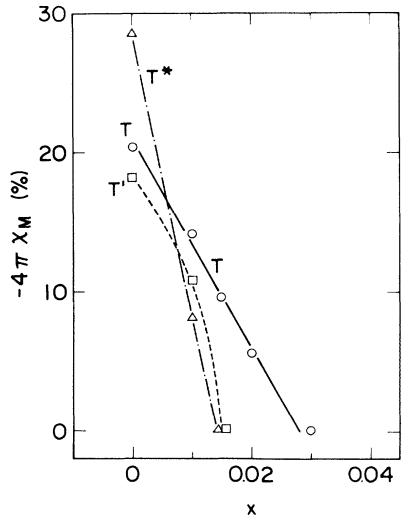


FIG. 4. Meissner signal at 5 K as a function of $x$ for $La_{1.85}Sr_{0.15}Cu_{1-x}Zn_xO_{4-\delta}$ ($T$), $Nd_{1.4}Ce_{0.2}Sr_{0.4}Cu_{1-x}Zn_xO_{4-\delta}$ ($T^*$) and $Nd_{1.85}Ce_{0.15}Cu_{1-x}Zn_xO_{4-\delta}$ ($T'$). All the curves are guides for the eyes.

tively. Note that both of these values are of the same order of magnitude as the Ginzburg-Landau coherence length. However, such a small-disk region isolated in the superconducting matrix may not be detected by shielding-effect measurements unless a large-scale clustering (larger than some thousands of regions) of Zn is formed. Another possible reason for the rapid decrease in the shielding signal as well as the Meissner signal is a rapid increase in the penetration depth up to the order of the grain size upon Zn doping. Such an increase in the penetration depth can be induced by a decrease in the average value of the spatially varying order parameter.[20] Thus, presently it is not clear how the normal-state portion extends in the sample upon Zn doping.

The reported $T_c$ values of the samples of $Nd_{1.85}Ce_{0.15}Cu_{1-x}Zn_xO_{4-\delta}$ in Refs. 11–14 were slightly higher than those of the present results. This discrepancy may be due to the difference in the uniformity of Zn distribution or to the difference in the reducing process employed for the sample preparation.

The temperature dependence of resistivity was measured in an applied field for the samples of the $T$ phase with $x=0$, 0.01, 0.02, and 0.03. Figures 6(a) and 6(b) show the resistive transitions for the samples with $x=0$ and 0.02, respectively. The resistive transition tail where the resistivity is less than $\frac{1}{4}$ of the normal-state resistivity develops significantly with increasing $H$. This is probably due to weak links formed in the samples or flux-creep dissipation. Excluding the tail portion, the shift of the transition curve with increasing $H$ is different for the samples

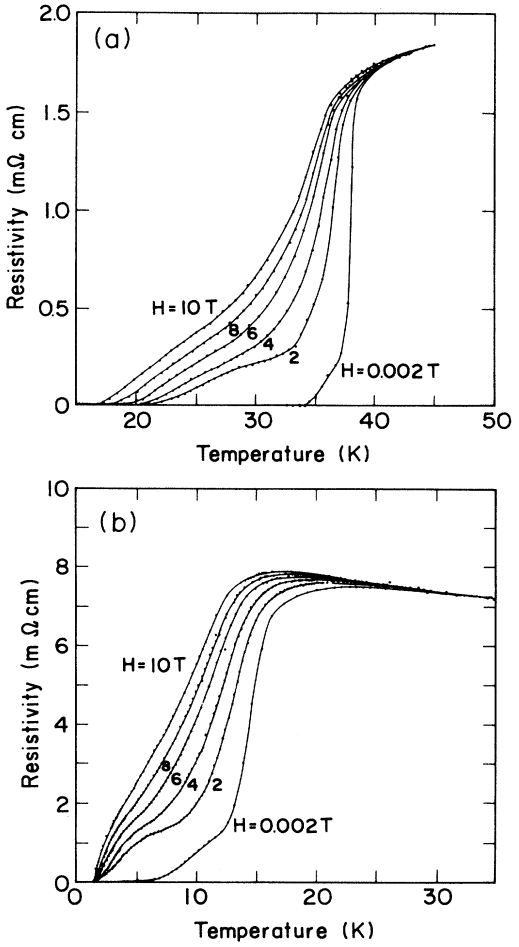


FIG. 6. Temperature dependence of electrical resistivity for the samples of (a) $La_{1.85}Sr_{0.15}CuO_{4-\delta}$ and (b) $La_{1.85}Sr_{0.15}Cu_{0.98}Zn_{0.02}O_{4-\delta}$ in various applied magnetic fields.

with $x=0$ and 0.02. For the sample with $x=0$, the onset temperature remains nearly constant, while it shifts for the sample with $x=0.02$ as $H$ increases. This suggests that the coherence length $\xi(0)$ for the sample with $x=0.02$ is longer than that of the sample with $x=0$.

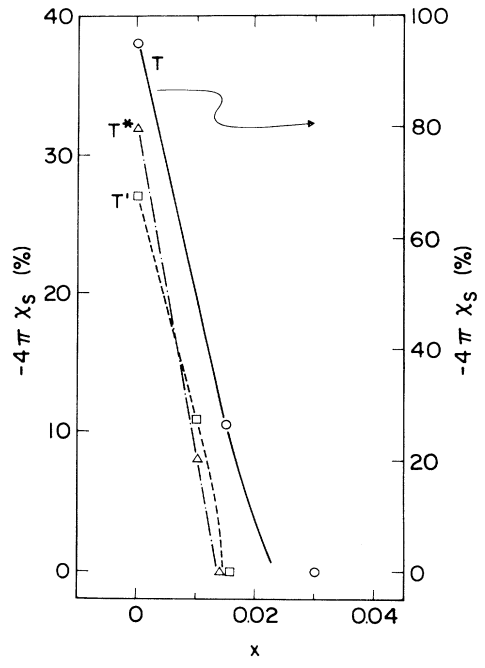


FIG. 5. Shielding signal at 5 K as a function of $x$ for $La_{1.85}Sr_{0.15}Cu_{1-x}Zn_xO_{4-\delta}$ ($T$), $Nd_{1.4}Ce_{0.2}Sr_{0.4}Cu_{1-x}Zn_xO_{4-\delta}$ ($T^*$), and $Nd_{1.85}Ce_{0.15}Cu_{1-x}Zn_xO_{4-\delta}$ ($T'$). All the curves are guides for the eyes.

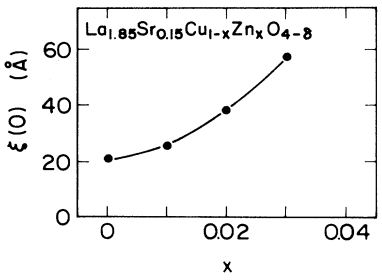


FIG. 7. The dependence of $\xi(0)$ on $x$ for $La_{1.85}Sr_{0.15}Cu_{1-x}Zn_xO_{4-\delta}$. The curve is a guide for the eyes.

There are some difficulties in the estimation of $\xi(0)$ from the upper critical field calculated using resistive transition curves because of flux-creep dissipation, flux-flow dissipation, and superconducting fluctuation. Suzuki and Hikita[21] reported for the $La_{2-y}Sr_yCuO_4$ system that the value of $\xi(0)$ estimated using $T_c(H)$ values at which resistivity was 70% of the normal-state resistivity agrees with that estimated from the field-dependent fluctuation conductivity. In the present work, we employ $T_c(H)$'s under applied fields at which resistivity was 70% of the normal-state resistivity. With the $T_c(H)$ values. $H_{c2}(0)$ and $\xi(0)$ are estimated using the relations

$$H_{c2}(0)=-0.69T_c(dH_{c2}/dT)_{T_c}=\phi_0/2\pi[\xi(0)]^2 .$$

Values estimated in this way for $\xi(0)$ are plotted with respect to the Zn content $x$ in Fig. 7. The $\xi(0)$ values increase as $x$ increases. In the BCS theory, $\xi(0)$ is inversely proportional to $T_c$. The decrease in the magnitude of $T_c$ with the Zn substitution should increase $\xi(0)$ within the framework of the BCS theory. If the doped Zn ions significantly reduce the carrier mean free path to the order of or less than $\xi(0)$, the length of $\xi(0)$ decreases with increasing $x$. However, we did not observe such an effect. Also, from the similar measurements for the $T'$ phase, we were not able to observe the shortening of $\xi(0)$ when Zn ions were doped.

### C. Magnetic properties in normal state

Zn substitution is expected to introduce spin vacancies in the two-dimensional antiferromagnetically (AF) correlated Cu spin system. In order to understand the effects of the spin vacancies, the temperature dependence of magnetic susceptibility for the $T$ compounds $La_{1.85}Sr_{0.15}Cu_{1-x}Zn_xO_{4-\delta}$ with $x=0$–$0.04$ was measured as shown in Fig. 8. Before analyzing the Zn-substitution effect, we first discuss the susceptibility of $La_{1.85}Sr_{0.15}CuO_{4-\delta}$. The measured susceptibility should consist of a contribution from the $3d$ spins and many other temperature-independent contributions such as the core diamagnetism and Van Vleck paramagnetism from the ion cores, and Pauli paramagnetism, Landau diamagnetism, and orbital contribution from the conduction electrons. The susceptibility of the sample with $x=0$ decreases with decreasing temperature as shown in Fig. 8. This behavior is probably due to the short-range two-dimensional antiferromagnetic correlations of $Cu^{2+}$ spins.[22,23]

Upon Zn doping, the Curie-Weiss component seems to be superposed on the two-dimensional (2D) AF susceptibility. In order to see this situation more clearly, we subtract the susceptibility of the Zn-free sample $\chi_n(0)$ from that of the sample containing Zn, $\chi(x)$. Note that $\chi_n(0)$ is defined as the normal-state susceptibility which excludes superconductivity diamagnetism by means of linear extrapolation of the data for the range of 60–130 to 0 K. Figure 9 shows the temperature dependence of

$$1/\chi_{Zn}(x)=1/[\chi(x)-\chi_n(0)]$$

with $x$ as a parameter. The temperature-independent

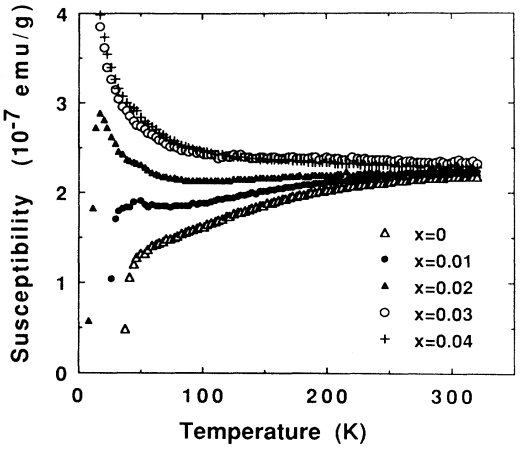


FIG. 8. Temperature dependence of the magnetic susceptibility of the normal state for the samples of $La_{1.85}Sr_{0.15}Cu_{1-x}Zn_xO_{4-\delta}$.

terms in susceptibility are considered not to be significantly affected by few percent of Zn substitution. Therefore, the susceptibility after subtracting $\chi_n(0)$ mainly consists of the $3d$ spin contribution induced by the Zn substitution. From Fig. 9, $\chi_{Zn}(x)$ appears to follow the Curie-Weiss law at temperatures below 150 K. The estimated effective Bohr magneton per Cu ($p_{eff}$) from Fig. 9 is plotted with respect to $x$ in Fig. 10 (solid circles). $p_{eff}$ increases linearly with increasing Zn content. A similar behavior of $p_{eff}$ was reported by $La_{1.85}Sr_{0.15}Cu_{1-x}Ga_xO_{4-\delta}$ by Cieplak *et al.*[24] The linear relation in Fig. 10 suggests that the doped Zn ions induce isolated Cu spins around them and the spins are governed by the Curie-Weiss law. If $1.9\mu_B$ is assumed to an isolated spin of $Cu^{2+}$ and the slope of the solid line in

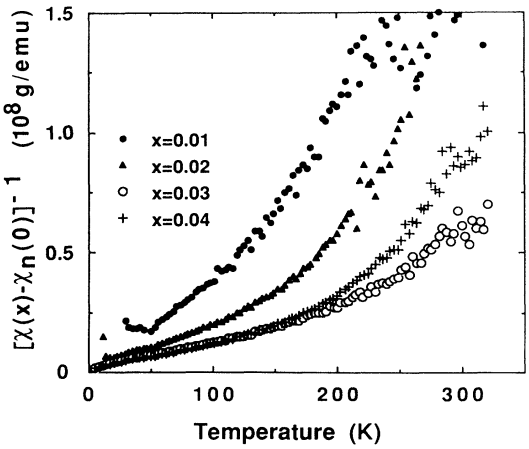


FIG. 9. Temperature dependence of the inverse susceptibility after subtraction of $\chi_n(0)$ for $La_{1.85}Sr_{0.15}Cu_{1-x}Zn_xO_{4-\delta}$ derived from Fig. 8.

Fig. 10 is employed, a single Zn ion can induce $2.2\pm0.3$ $Cu^{2+}$ spins.

ESR measurements were made for the same $T$-phase samples to detect the isolated Cu spins. An ESR signal was not observed for any sample with $x=0$–$0.03$. In the cuprate superconductors as well as $La_2CuO_4$, the ESR signals are not detected.[25] One of the possible reasons is that the relaxation of Cu spins is too fast compared with the microwave frequency.[26] The same mechanism may work for the present Zn-doped samples. We estimate from our ESR results that the amount of paramagnetic impurities is less than 0.1%.

Normal-state susceptibility was measured for another set of samples which were sintered at 1080 °C that was slightly higher than the sintering temperature employed previously. The magnitude of resistivity of these samples is lower (0.9–1.6 mΩ cm at room temperature) than that of the samples previously studied. The effective Bohr magnetons per Cu, $p_{\rm eff}$, for these samples are plotted in Fig. 10 using open circles. The two sets of data are in reasonable agreement as seen in Fig. 10. Therefore, the superposition of the Curie-Weiss term due to Zn substitution on the $\chi_n(0)$ term is probably not caused by precipitation of paramagnetic impurity phases.

Substituted $Zn^{2+}$ for the Cu site might play a role of "spin vacancy" and therefore weaken the AF correlation around a Zn ion in the $[CuO_2]$ plane. The AF correlation can also be weakened by heavily doped carriers. Takagi *et al.*[22] and Torrance *et al.*[23] reported that, when $y$ exceeded 0.15 for $La_{2-y}Sr_yCuO_4$, susceptibility increased and a peak appeared for the temperature dependence of susceptibility at a temperature below 400 K. The peak temperature $T_{\rm max}$ was calculated to be $0.94J/k_B$ in the simplest model,[27] where $J$ was exchange-coupling energy between $Cu^{2+}$ spins. As $y$ increases, $T_{\rm max}$ decreases below 300 K before superconductivity vanishes. In the case of Zn doping, the peak is not observed in the temperature range below 320 K even for the nonsuperconducting samples. In this case, superposition of a Curie-Weiss term on $\chi_n(0)$ is observed instead of a peak. The AF correlation is weakened differently depending on the dopant, i.e., Zn or holes. In the case of hole doping, the AF correlation may be weakened by a mean field due to the doped holes. Contrary to this, Zn ions presumably destroy local AF correlations. This is the reason why we consider the local destruction of superconductivity around a doped Zn ion in Sec. III B. It should be noted that the effective Bohr magneton per Zn is estimated to be $(0.96\pm0.14)\mu_B$ and is nearly independent of $x$, as reported by Xiao *et al.*[28] This supports the local destruction model. The recent work by Yoshizaki *et al.*[29] for $La_{2-y}Sr_yCu_{1-x}Zn_xO_{4-\delta}$, where $y=0.18$ and 0.2 showed that the $T_{\rm max}$ decreased with increasing Zn concentration. This suggests that the local destruction of the AF correlation leads to a decrease in the average value of $J$.

Figure 11 shows the temperature dependence of magnetic susceptibilty for $Nd_{1.4}Ce_{0.2}Sr_{0.4}CuO_{4-\delta}$ and $Nd_{1.85}Ce_{0.15}CuO_{4-\delta}$. The maximum change in susceptibilty due to Zn doping is less than 2%. The effective Bohr magneton per Nd ion estimated from the data in the temperature range above 80 K is $(3.50\pm0.04)\mu_B$ for all the samples of the $T^*$ and $T'$ phases. This estimated value is in good agreement with that known for a free $Nd^{3+}$ ion, i.e., $3.50\mu_B$. Therefore, the data appear to represent the contribution from the $Nd^{3+}$. It is not possible to detect the Zn-substitution effect on Cu spins because the susceptibility of $Nd^{3+}$ was too strong compared with this effect. However, it may be supposed that doped Zn ions destruct local AF correlations of the Cu spin system in the $T^*$ and $T'$ phases also, as was in the case of the $T$ phase. At temperatures below 30 K, susceptibility deviated from the Curie-Weiss behavior for all the samples. This may be due to an interaction of $4f$ moments of $Nd^{3+}$ and $3d$ moments of $Cu^{2+}$, as was proposed for $Nd_2CuO_4$.[10]

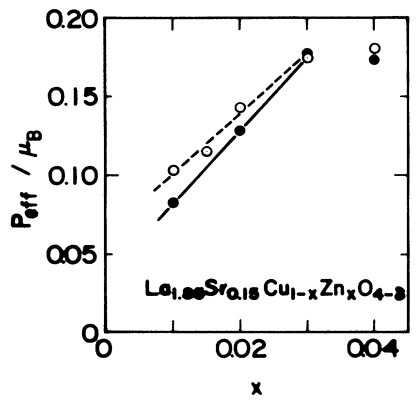


FIG. 10. The dependence of effective Bohr magneton per Cu on $x$ for $La_{1.85}Sr_{0.15}Cu_{1-x}Zn_xO_{4-\delta}$. The data for two different sample sets are indicated by solid circles and open circles. The lines are guides for the eyes.

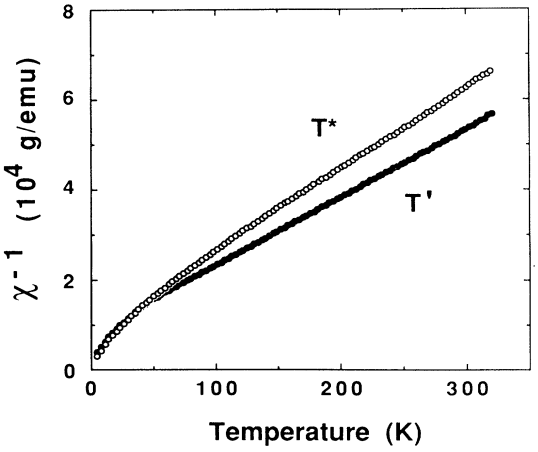


FIG. 11. Temperature dependence of inverse susceptibility for the samples of $Nd_{1.4}Ce_{0.2}Sr_{0.4}CuO_{4-\delta}$ ($T^*$) and $Nd_{1.85}Ce_{0.15}CuO_{4-\delta}$ ($T'$).

### D. Hall coefficient

Figure 12 shows the temperature dependence of Hall coefficients $R_H$ for Zn-doped $T$-phase samples. $R_H$ for the sample with $x=0$ increases with decreasing temperature, as previously reported.[22] Upon Zn substitution, $R_H$ does not drastically change compared with $T_c$ but decreases monotonically. Note that, for all Zn-doped samples, the $R_H$-versus-$T$ curves exhibit maxima around 60 K. The temperature dependence of $R_H$, $dR_H/dT$, derived from the $R_H$-versus-$T$ data in the temperature range between 90 and 300 K are depicted in Fig. 13. $|dR_H/dT|$ decreases as $x$ increases. Clayhold *et al.*[30] reported that, as the amount of dopant (Ni) $x$ increases, both $T_c$ and $|dR_H/dT|$ are reduced in $La_{1.85}Sr_{0.15}Cu_{1-x}Ni_xO_{4-\delta}$. They pointed out that the strong temperature dependence of $R_H$ was probably intrinsic to high-$T_c$ instability.[30] In Fig. 13, a similar behavior is observed for $La_{1.85}Sr_{0.15}Cu_{1-x}Zn_xO_{4-\delta}$, although the change in $R_H$ upon Zn doping is opposite to the case of Ni doping.

In spite of the expectation that the Zn substitution does not affect the carrier concentration (per unit volume), the Hall number $n_H(=1/eR_H)$ appears to increase with increasing Zn content. The valence state of a doped Zn in the $T$ phase was confirmed to be 2+ by an XPS experiment.[17] From the iodometric titration results for $La_{1.85}Sr_{0.15}Cu_{1-x}Zn_xO_{4-\delta}$ with $x=0$, 0.02, and 0.03, the oxygen deficiency $\delta$ for each sample is found not to be altered upon Zn doping. That is, $\delta$'s are $0.01\pm0.01$. Therefore, the density of chemically doped holes per unit area of the $[(Cu,Zn)O_2]$ plane is not changed by Zn substitution. UPS measurements were also done for the $T$ samples with $x=0$, 0.01, 0.02, and 0.03. A "Fermi-edge"-like structure is observed for all the samples. The shape of the "Fermi-edge" and the density of state at $E_F$ are not significantly changed by Zn doping.[17] These observations are consistent with the fact that the concentration of chemically doped holes is not changed by Zn doping.

Concerning the $T'$-phase samples, $R_H$ is depicted in Fig. 14. Each curve exhibited a broad peak around 120 K, as previously reported.[15,31] The absolute value of $R_H$ decreases upon Zn substitution (except for the data in the temperature range below 60 K). The oxygen contents analyzed by an inert gas fusion nondispersive ir method

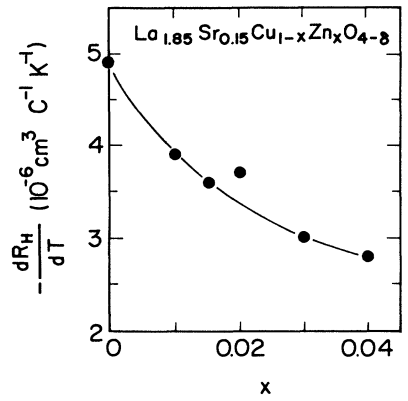


FIG. 13. The dependence of the slope $dR_H/dT$ on $x$ for $La_{1.85}Sr_{0.15}Cu_{1-x}Zn_xO_{4-\delta}$. The curve is a guide for the eyes.

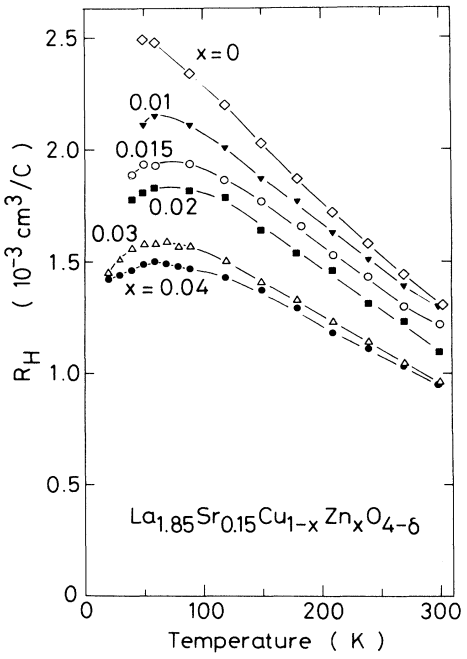


FIG. 12. Temperature dependence of Hall coefficient $R_H$ for the samples of $La_{1.85}Sr_{0.15}Cu_{1-x}Zn_xO_{4-\delta}$. All the curves are guides for the eyes.

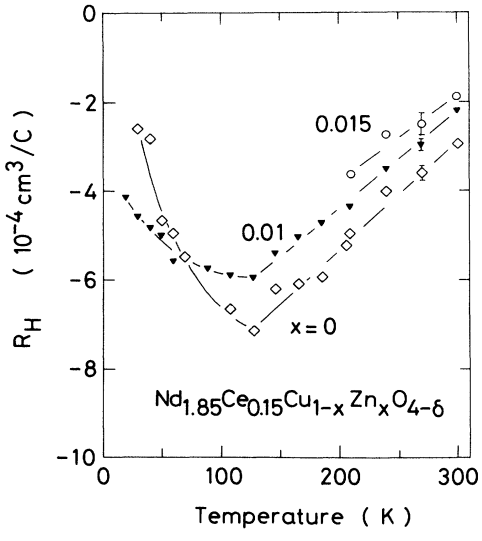


FIG. 14. Temperature dependence of Hall coefficient $R_H$ for the samples of $Nd_{1.85}Ce_{0.15}Cu_{1-x}Zn_xO_{4-\delta}$. All the curves are guides for the eyes.

remain constant within ±1% for the samples of $Nd_{1.85}Ce_{0.15}Cu_{1-x}Zn_xO_{4-\delta}$ with $x=0-0.04$. From the XPS measurements, the valence of a Ce ion seems not to be changed by Zn doping.

If Zn provides carriers of a fixed sign (i.e., either positive or negative) into the $[CuO_2]$ planes of both the $T$ and $T'$ phases, $R_H$'s for the two different type phases should depend on the Zn concentration in a parallel manner. However, this speculation does not agree with the present experimental results. For both the $T$ and $T'$ phases, the absolute values of $R_H$ decrease as the Zn concentration increases, although the concentrations of the chemically doped carriers remain constant. This, together with the fact that the slope of the $R_H$-versus-temperature curve decreases as $x$ increases (Fig. 13) suggest that the overall electronic state is somewhat altered by Zn substitution. The discrepancy in the carrier concentrations of chemically doped carriers and the Hall number $n_H$ for both the $T$ and $T'$ phases was pointed out by Uchida, Takagi, and Tokura.[9] When mobile carriers are doped by substitution of Sr or Ce in $La_2CuO_4$ or $Nd_2CuO_4$, the measured value of $R_H$ agrees at the initial stage of doping with that calculated for chemical doping using a rigid-band model which has an energy gap. However, with doping higher than 5%, $R_H$ deviates from the expectation for chemical doping. This has been interpreted as a transition from a rigid-band model to a Fermi-liquid model.[9] Consequently, it may be suggested that the Zn substitution does not affect the level due to chemical doping but enhances the shift of the system from a rigid-band model (with a gap) towards a Fermi-liquid model. The deterioration of the AF correlation by Zn doping (mentioned in Sec. III C) may cause such a shift in the electronic state. This shift in the electronic state may cause the reduction of $T_c$.

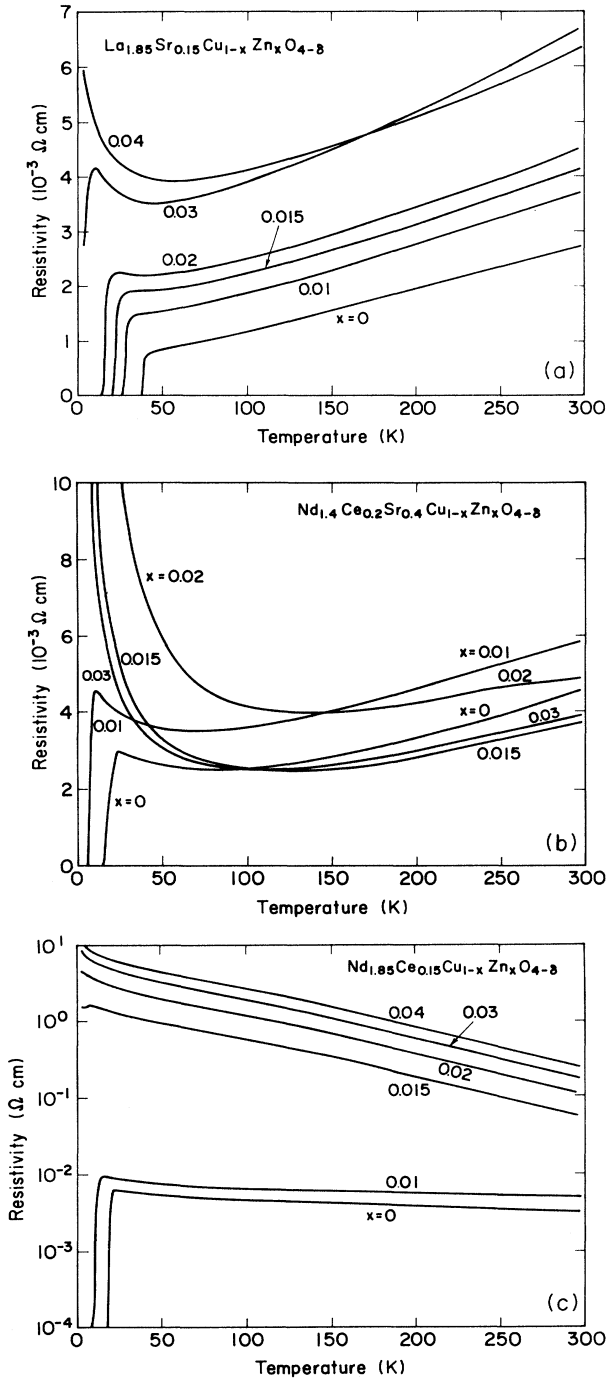


FIG. 15. Temperature dependence of electrical resistivity for the samples of (a) $La_{1.85}Sr_{0.15}Cu_{1-x}Zn_xO_{4-\delta}$. (b) $Nd_{1.4}Ce_{0.2}Sr_{0.4}Cu_{1-x}Zn_xO_{4-\delta}$, and (c) $Nd_{1.85}Ce_{0.15}Cu_{1-x}Zn_xO_{4-\delta}$.

For the $T^*$ phases, $R_H$ above 150 K was not changed by Zn doping. Below 150 K the slope of the $R_H$-versus-temperature curves decreased with increasing Zn concentration.[32] This result indicated that Zn doping in the $T^*$ sample also did not significantly change the hole concentration, but altered the electronic states.

Finally, we show the results of resistivity measurements in Fig. 15 as a function of temperature. In the $T'$ phase [Fig. 15(c)], resistivity increases drastically with increasing $x$. The reason for the resistivity increase while the carrier concentration remains constant is unknown. The resistivity of single crystal $Nd_{1.84}Ce_{0.16}Cu_{4-\delta}$ was reported to be lower than that of ceramic samples and metallic at temperatures between $T_c$ and 300 K.[33] Hence, the resistivity of ceramic samples may not represent the intrinsic value for the material. On the other hand, for the $T$-phase [Fig. 15(a)] and $T^*$-phase [Fig. 15(b)] samples, room-temperature resistivity was not changed by Zn substitution. In fact, for the $T$ samples which were sintered at 1080 °C, slightly higher than the sintering temperature for those samples whose data are shown in Fig. 15(a), the magnitudes of resistivity at 300 K for all the samples ($x=0-0.04$) are nearly identical, being in the range of 0.9–1.6 m Ω cm. If the number of mobile carriers increased due to Zn doping, resistivity would decrease, as was the case of high Sr doping into $La_{2-y}Sr_yCuO_4$. If the doped Zn ions significantly scattered the mobile carriers, the resistivity would increase upon Zn doping. No such effects are observed in the present work. It should be noted that the appearance of a minimum in the resistivity-versus-temperature curve at low temperatures (below 50 and 150 K for the $T$ and $T^*$

phases, respectively) is observed for Zn-doped $T$- and $T^*$-phase samples. This indicates that the mobility of holes at low temperatures is decreased by Zn doping.

## IV. SUMMARY

The effects of substitution of Zn for Cu in superconducting cuprates of the $T$, $T^*$, and $T'$ structures were investigated. The dependence of the lattice parameters on the Zn concentration is parallel for the $T$ and $T^*$ samples, while, for the $T'$ samples, it is different. For the $T$ and $T^*$ samples, the $a$ axis increases and the $c$ axis decreases as the Zn concentration increases. On the contrary, for the $T'$ samples, both the $a$ and $c$ axes remain nearly constant when the Zn concentration is increased. The Zn substitution for Cu is found to suppress, in a similar way, the magnitude of $T_c$, the Meissner signal, and the shielding signal for the $T$, $T^*$, and $T'$ cuprate superconductors. The decrease in the Meissner signal with increasing Zn content is not attributed to an increase in the macroscopic pinning force. Using the magnetoresistance data and the Werthamer-Helfand-Hohenberg relation, $H_{c2}$ was obtained and the coherence length was estimated for each of the $T$-phase samples. The obtained coherence length is in good agreement with $\xi(0)$ calculated using the relation $\xi(0) \propto 1/T_c$. The estimated $\xi(0)$ suggests that the electron mean free path is not significantly decreased by Zn substitution. Hall coefficients were measured for the $T$ and $T'$ samples. As Zn content increases, the absolute value of $R_H$ slightly decreases for both the $T$ and $T'$ phases and the slope of the $R_H$-versus-$T$ curve decreases for the $T$ phase, but the chemical doping level remains nearly constant. The Hall effect data suggests that, assuming the doped Zn ions play the same role in the electronic structures of both the $T$ and $T'$ phases, they provide the samples with neither holes nor electrons. From the magnetic susceptibility for the $T$ phase, the isolated spins of Cu induced around Zn was estimated. The decrease in $|R_H|$ upon Zn doping may be related to the destruction of local AF correlations around each Zn ion in the $T$ and $T'$ phases.

## ACKNOWLEDGMENTS

We would like to thank Y. Yamada of Superconductivity Research Laboratory for his help in ESR measurements and stimulating discussions. We also thank Professor K. Kitazawa and Dr. S. Kambe of the University of Tokyo, and M. Kosuge of Superconductivity Research Laboratory for helpful discussions.

---

*Present address: Advanced Research Laboratory, Toshiba Research and Development Center, 1, Komukai Toshiba-cho, Saiwai-ku, Kawasaki, 210, Japan.

[1]R. J. Birgeneau, D. R. Gabbe, H. P. Jenssen, M. A. Kastner, P. J. Picone, T. R. Thurston, G. Shirane, Y. Endoh, M. Sato, K. Yamada, Y. Hidaka, M. Oda, Y. Enomoto, M. Suzuki, and T. Murakami, Phys. Rev. B **38**, 6614 (1988).

[2]J. M. Tarascon, L. H. Greene, P. Barboux, W. R. McKinnon, G. W. Hull, T. P. Orland, K. A. Delin, S. Foner, and E. J. McNiff, Jr., Phys. Rev. B **36**, 8393 (1987).

[3]N. Okazaki, S. Kambe, A. Kishi, N. Kanazawa, A. Ohtomo, A. Fukuoka, T. Hasegawa, K. Kishio, K. Kitazawa, and K. Fueki (unpublished).

[4]A. Maeda, T. Yabe, S. Takebayashi, M. Hase, and K. Uchinokura, Phys. Rev. B **41**, 4112 (1990).

[5]M. W. Shafer, T. Penny, B. L. Olsen, R. L. Greene, and R. H. Koch, Phys. Rev. B **39**, 2914 (1989).

[6]G. Xiao, A. Bakhshai, M. Z. Cieplak, Z. Tesanovic, and C. L. Chien, Phys. Rev. B **39**, 315 (1989).

[7]J. Akimitsu, S. Suzuki, M. Watanabe, and H. Sawa, Jpn. J. Appl. Phys. **27**, L1859 (1988).

[8]Y. Tokura, H. Takagi, and S. Uchida, Nature **337**, 345 (1989).

[9]S. Uchida, H. Takagi, and Y. Tokura, Physica C **162-164**, 1677 (1989).

[10]Y. Endoh, M. Matsuda, K. Yamada, K. Kakurai, Y. Hikada, G. Shirane, and R. J. Birgeneau, Phys. Rev. B **40**, 7023 (1989); T. R. Thurston, M. Matsuda, K. Kakurai, K. Yamada, Y. Endoh, R. J. Birgeneau, P. M. Gehring, Y. Hikada, M. A. Kastner, T. Murakami, and G. Shirane, Phys. Rev. Lett. **65**, 263 (1990).

[11]C. Barlingay, V. Garcia-Vazquez, C. M. Falco, S. Mazumdar, and S. H. Risbud, Phys. Rev. B **41**, 4797 (1990).

[12]J. M. Tarascon, E. Wang, S. Kivelson, B. G. Bagley, G. W. Hull, and R. Ramesh, Phys. Rev. B **42**, 218 (1990).

[13]I. Felner, D. Hechel, and U. Yaron, Physica C **165**, 247 (1990).

[14]G. Hilscher, S. Pollinger, M. Forsthuber, N. Pillmayr, K. Remschnig, P. Rogl, M. Reissner, W. Steiner, and P. Knoll, Physica C **167**, 472 (1990).

[15]H. Takagi, S. Uchida, and Y. Tokura, Phys. Rev. Lett. **62**, 1197 (1989).

[16]A. I. Nazzal, V. Y. Lee, E. M. Engler, R. D. Jacowitz, Y. Tokura, and J. B. Torrance, Physica C **153-155**, 1367 (1988).

[17]R. Itti, S. Ikegawa, K. Ikeda, H. Yamauchi, N. Koshizuka, and S. Tanaka (unpublished).

[18]*Powder Diffraction File of the Joint Committee on Powder Diffraction Standards* (International Center for Diffraction Data, Swarthmore, PA, 1988).

[19]K. Kitazawa, O. Nakamura, T. Matsushita, Y. Tomioka, N. Motohira, M. Murakmi, and H. Takei, in *Proceedings of the Second International Symposium on Superconductivity, Tsukuba, Japan, 1989,* edited by T. Ishiguro and K. Kajimura (Springer-Verlag, Tokyo, 1990), p. 609.

[20]A. Junod, D. Eckert, T. Graf, G. Triscone, and J. Muller, Physica C **162-164**, 1401 (1989).

[21]M. Suzuki and M. Hikita, Jpn. J. Appl. Phys. **28**, L1368 (1989).

[22]H. Takagi, T. Ido, S. Ishibashi, M. Uota, S. Uchida, and Y. Tokura, Phys. Rev. B **40**, 2254 (1989).

[23]J. B. Torrance, A. Bezinge, A. I. Nazzal, T. C. Huang, S. S. P. Parkin, D. T. Keane, S. J. LaPlaca, P. M. Horn, and G. A. Held, Phys. Rev. B **40**, 8872 (1989).

[24]M. Z. Cieplak, G. Xiao, A. Bakhashi, and C. L. Chien, Phys. Rev. B **39**, 4222 (1989).

[25]F. Mehran, S. E. Barnes, G. V. Chandrashekhar, T. R. McGuire, and M. W. Shafer, Solid State Commun. **67**, 1187 (1988).

[26]F. Mehran and P. W. Anderson, Solid State Commun. **71**, 29 (1989).
[27]M. E. Lines, J. Phys. Chem. Solids **31**, 101 (1970).
[28]G. Xiao, M. Z. Cieplak, J. Q. Xiao, and C. L. Chien, Phys. Rev. B **42**, 8752 (1990).
[29]R. Yoshizaki, N. Ishikawa, H. Sawada, E. Kita, and A. Tasaki, Physica C **166**, 417 (1990).
[30]J. Clayhold, N. P. Ong, Z. Z. Wang, J. M. Tarascon, and P. Barboux, Phys. Rev. B **39**, 7324 (1989).
[31]S. Ikegawa, M. Kosuge, T. Wada, A. Ichinose, Y. Yaegashi, K. Nakao, T. Yamashita, T. Sakurai, and H. Yamauchi, in *Proceedings of the Second International Symposium on Superconductivity, Tsukuba, Japan, 1989,* edited by T. Ishiguro and K. Kajimura (Springer-Verlag, Tokyo, 1990), p. 517; S. Ikegawa, T. Wada, A. Ichinose, T. Yamashita, T. Sakurai, Y. Yaegashi, T. Kaneko, M. Kosuge, H. Yamauchi, and S. Tanaka, Phys. Rev. B **41**, 11 673 (1990).
[32]S. Ikegawa, Y. Yamashita, T. Wada, H. Yamauchi, and S. Tanaka (unpublished).
[33]Y. Hidaka and M. Suzuki, Nature 338, 635 (1989).